JOURNAL OF MATERIALS SCIENCE **34** (1999) 1523–1531

The effect of calcination on the microstructural characteristics and photoreactivity of Degussa P-25 TiO_2

JOHN F. PORTER*, YU-GUANG LI‡, CHAK K. CHAN
Hong Kong University of Science and Technology, Department of Chemical Engineering, Hong Kong, People's Republic of China
E-mail: kejep@ust.hk

Changes in the microstructural characteristics of Degussa P-25 titania as a result of calcination have been studied using XRD, BET and TEM. The photocatalytic activities of the samples were also examined using the degradation of phenol as a model reaction. The results indicate firstly that calcination significantly affects both microstructural characteristics and photoactivity and secondly that there is an apparent relationship between photocatalytic activity and certain microstructural characteristics. Over the range of calcination temperatures and durations studied, the sample calcined at 923 K for 3 hours revealed the highest photoreactivity, which can be ascribed to an improvement in crystallinity on calcination. The increase in the rutile content and grain growth caused by the calcination at higher temperatures were observed to decrease the photocatalytic activities of the TiO_2 samples.

1. Introduction

Nanocrystalline TiO_2 heterogeneous photocatalysis has recently been the subject of many studies in the field of environmental protection. The process of the photocatalytic degradation of organic pollutants by the semiconductor powders has been considered to be very promising because of its non-toxicity, low cost and high activity [1, 2]. However, if it is to be used practically, photocatalytic efficiency needs to be improved. In particular, TiO_2 samples prepared and treated by different methods exhibit a great variety in photocatalytic efficiency even though they have the same crystal form [3–5]. Commercial samples have also been shown to exhibit photocatalytic activities that can vary from batch to batch [1], since photocatalytic properties may be influenced by physicochemical variables, including particle size, surface area, surface crystallinity and the state of surface hydration. For example, the activity of the rutile phase has been found to vary with preparation conditions [5].

For photocatalytic reactions, it is quite common for authors to use Langmuir-Hinshelwood kinetic expressions to model reaction data [6–8], indicating the importance of substrate preadsorption and thus surface area. Studies do not conclusively support this interpretation however [9] and a clear relationship between surface area and photocatalytic activity has not been demonstrated for photocatalysis by TiO_2 [5].

The size of TiO_2 particles has been demonstrated to influence their photocatalytic activity, although there appears to be some disagreement in that Rivera *et al*. observed that the photocatalytic degradation rate increases linearly with increasing anatase crystallite size [3] whereas Anpo *et al*. have reported that for anatase particles in the range of 4–50 nm, photocatalytic activity increased with decreasing TiO_2 particle diameter, an observation which they attributed to size quantization [10].

It seems obvious that a fundamental understanding of the factors affecting photocatalytic is necessary to make more efficient use of existing catalysts and provide design criteria for new catalyst preparation, thus it remains a subject of great interest. Since commercial Degussa P-25 TiO_2 is commonly used as a basis for comparison with TiO_2 photocatalysts prepared by other procedures, a study of those microstructural features relevant to the photoreactivity of P-25 TiO_2 and how they are affected by calcination should prove useful to developing a better understanding of the effect of sample physicochemistry on photocatalytic reactivity. Thus this paper focuses on a detailed study of the sintering characteristics and photoreactivities of calcined P-25 TiO_2 by using XRD, TEM, BET and photocatalytic degradation.

*Author to whom all correspondence should be addressed.
‡*Current address*: Department of Chemistry, Zhongshan University, Guangzhou, People's Republic of China.

2. Materials and methods

2.1. Catalyst and treatment

Commercial Degussa P-25 TiO_2 was used as supplied. Samples were heat treated in a conventional muffle furnace at 873, 923, 973, 1023, 1073, 1173 and 1273 K for three hours. Some samples were calcined for extended durations of six and twenty-four hours at 873 K to examine the effect of calcination time. Both the calcined titania samples and the original Degussa P-25 powder then underwent physical characterisation as well as evaluation of their photocatalytic performance.

2.2. Catalyst characterisation

Powder X-ray diffraction (XRD) was used for crystal phase identification, estimation of the anatase to rutile ratio and of the crystallite size of each phase present. XRD patterns were obtained at room temperature with a Philips PW1831 diffractometer using CuK_α radiation. The primary particle size was estimated directly from Transmission Electron Microscopy (TEM) micrographs of powder samples. For TEM analysis, samples were prepared by dispersing the powders in methanol and allowing a drop of the resultant suspension to dry on a carbon support film covering a standard copper grid. TEM observations were carried out using a JEOL JEM-2010 Electron microscope. A quantitative study of the specific surface area, total porosity and pore size was performed using a Micromeritics ASAP 2000 nitrogen adsorption apparatus.

2.3. Photocatalytic evaluation

All the experiments were carried out using the same cylindrical annular batch photoreactor. The reactor has an internal volume of 2 l with the UV lamp positioned on the axis inside a quartz immersion well. Illumination was provided by a 400 W medium pressure mercury lamp (Phillips HPA 400/30s) held in the immersion wall and cooled by air at a flowrate of 20–40 l/min, depending on the ambient temperature. The light intensity after passing through both the filled cooling jacket and reaction suspension was continuously monitored at a wavelength of 365 nm using a radiometer (Vilber Lourmat CX-365) in a fixed position corresponding to the centre of the lamp. The intensity after passing through pure water was measured to be 48 mW/cm^2. The reactor was maintained at isothermal condition by passing chilled water through the cooling jacked of the immersion well. Oxygen was continuously sparged through a porous glass frit at the bottom of the reactor at a fixed flow rate of 1 l/min. A schematic of the photoreactor is shown in Fig. 1.

For the degradation experiments, between 0.15 and 1.0 g of the selected TiO_2 sample was suspended in 1.5 l of ultra-pure water. Phenol was selected as a model pollutant for the photocatalytic degradation experiments because it is a non-volatile, common contaminant in industrial wastewater. The initial concentration of phenol in dispersion was fixed at 40 mg/l and the initial pH of the dispersion was adjusted to 3.0 by the addition of sulphuric acid [5]. Both were monitored periodically thereafter. All experiments were

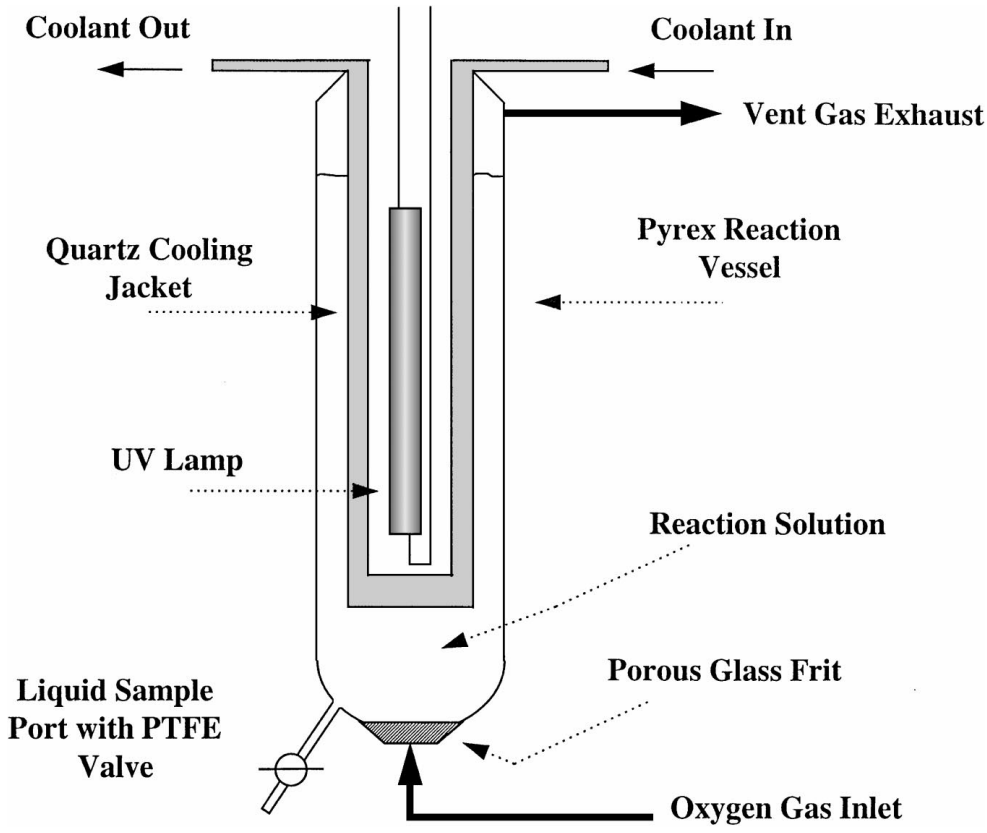

Figure 1 Schematic of the annular batch photocatalytic reactor.

performed at a solution temperature of 300 K for a reaction time of 150 min, with samples being taken for analysis every 15 min. Since the overall goal of the water treatment process was the complete destruction of the organic pollutant—i.e. conversion to carbon dioxide, water and the oxidised inorganic anions of any heteroatoms present [11]—the rate of disappearance of Total Organic Carbon (TOC) was considered a key performance indicator and a Shimadzu TOC-500 analyser was used to determine the extent of mineralization in the samples.

3. Results and discussion

3.1. The effect of calcination on the microstructure of P-25 TiO_2

3.1.1. The variation of crystal composition with calcination

Fig. 2 illustrates the X-ray diffraction (XRD) patterns of the samples before and after calcination. The XRD pattern of the parent P-25 TiO_2 powder in Fig. 2 reveals the peaks of anatase (101) and rutile (110) at $2\theta = 25.4^\circ$ and 27.5° respectively, indicating that the bulk P-25 TiO_2 composition is a mixture of rutile and anatase. Based on the respective peak intensities, the rutile content in the original powder of P-25 TiO_2 can be calculated from the following Equation [12]:

$$x = \left(1 + 0.8\frac{I_A}{I_R}\right)^{-1} \quad (1)$$

where x is the weight fraction of rutile in the powders, while I_A and I_R are the X-ray intensities of the anatase and the rutile peaks respectively. The result indicates that there is 23.5% rutile, which is intermediate of the values presented by Beck *et al*. (25%) [13] and by Bickley *et al*. (20%) [14]. Calcination at 873 K for both 3 and 6 hours (samples 2 and 3) resulted in virtually no change in the relative intensity of both peaks, while after calcination for 24 hours (sample 4) the rutile content increased to 38.1%. This indicates that the transition of anatase to rutile is slow at a calcination temperature of 873 K. On increasing the temperature to over 973 K, the intensity of the rutile peak significantly increased while that of anatase peak decreased. For TiO_2 calcined at 1073 K for 3 hours (sample 8), the anatase peak disappeared. These features are consistent with the observations that the transition of anatase to rutile is immeasurably slow for calcination below 800 K, but is rapid at temperatures exceeding 1000 K [14]. An earlier study on the kinetics of the anatase-rutile transformation has shown that the transformation involves an overall contraction or shrinking of the oxygen structure and a co-operative movement of ions. The transformation needs to overcome both a strain energy for the oxygen ions to reach their new configuration and the energy necessary to break the Ti-O bonds as the titanium ions redistribute [15]. A high activation energy is required for this process (over 420 kJ/mol) and so the phase transition takes place only at a high temperatures. The rutile content of all the samples have been listed in Table I and clearly, it rapidly increases under calcination at temperatures greater than 923 K.

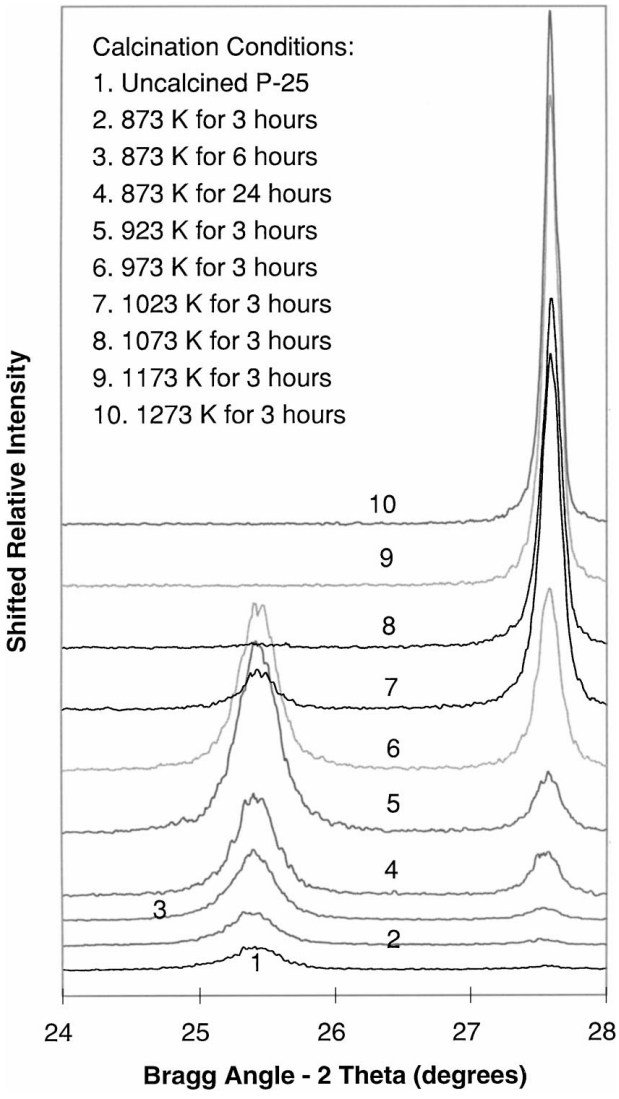

Figure 2 Effect of calcination on the crystal structure of Degussa P-25.

TABLE I XRD and TEM results for heat treated and raw Degussa P-25

Calcination conditions		Percent rutile	Crystallite size[a] (nm)		Primary particle size (nm)
Temp. (°C)	Time (h)		Anatase	Rutile	
0	0	23.3 ± 1.7	20.6	14.4	15–25
600	3	24.1 ± 2.1	22.9	17.9	15–25
600	6	24.0 ± 2.3	23.6	25.9	—
600	24	38.1 ± 1.8	25.9	28.7	20–40
0	0	23.3 ± 1.7	20.6	14.4	15–25
600	3	24.1 ± 2.1	22.9	17.9	15–25
650	3	28.7 ± 1.2	26.7	34.8	—
700	3	55.6 ± 2.0	30.8	51.9	30–50
750	3	91.2 ± 2.0	38.2	75.9	—
800	3	97.3 ± 1.5		129.3	100–200
900	3	99.3 ± 1.0			200–300
1000	3	99.5 ± 0.5			200–400

[a] Determined using Scherrer's equation (applicable from 3–200 nm).

3.1.2. The variation of crystallite size and crystallinity

Phase transformation is generally accompanied with crystal growth. The crystallite size can be determined from the broadening of corresponding X-ray spectral peaks by Scherrer's formula [16]:

$$L = \frac{K \cdot \lambda}{\beta \cdot \cos\theta} \tag{2}$$

where L is the crystallite size, λ is the wavelength of the X-ray radiation, K is usually taken as 0.94, β is the line width at half maximum height. The line width, β, was corrected for instrumental broadening by employing the patterns obtained for large-sized rutile TiO_2 under the same experimental conditions. The crystallite sizes of each phase present in the samples are listed in Table I. From the results we can see that a small increase in the anatase crystallite size was observed after calcination at temperatures below 923 K. Over 973 K, the increase becomes more obvious, however, a much more significant increase in crystallite size was observed for rutile. For example, at 1023 K (sample 7) the size of the anatase crystallites doubled whereas the rutile size increased by a factor of five.

Fig. 3 shows TEM micrographs of several samples. The TEM image of the original P-25 TiO_2 confirms the 15–25 nm size range of the primary particles. At a calcination temperature of 873 K, there is little increase in crystallite size over the original P-25 for up to 6 hours and only minor grain growth was observed even after calcination for 24 hours. Rapid grain growth began at 973 K, accelerated with temperature and, by 1173 K, the grain size had increased by a factor of 10. Indeed, mere visual inspection showed that after calcination at 1073 K for 3 hours the fine commercial powder samples became densified aggregates. Hence, at temperatures above 973 K, phase transformation and grain growth appear to occur simultaneously.

Hague *et al*. have presented a model for the phase transformation and crystal growth process of nanocrystalline titania [17]: as a sample is calcined at approximately 873 K, anatase crystals within agglomerates become sintered, thus the crystals grow through coalescence—transforming the original agglomerate into a single anatase grain. At the same time rutile nuclei begin to form and grow through the anatase matrix. Once the anatase-rutile transformation is complete, the rutile grain size is much larger than the original agglomerate and no longer nanocrystalline. A previous model developed by Edelson and Glaeser [18] proposed that intra-agglomerate densification and grain growth occur relatively rapidly compared to interagglomerate densification. The results presented here appear to be consistent with both models. The observation that rutile crystallites grow much more rapidly than anatase at high temperatures suggests that a qualitative interpretation of the relative order of the rates of the three processes would be: intra-agglomerate densification > anatase to rutile transformation > interagglomerate densification.

Of special interest is the variation of crystallinity with calcination. It is generally believed that the sharper the peak shape the higher is the crystallinity. For an improvement in crystallinity to be evident, XRD results should show that the peak height and the signal to noise ratio increase. From the XRD patterns of P-25 TiO_2 before and after calcination, shown in Fig. 2, a definite change in the peak shape was observed. For example, the peak shape of anatase in samples 2 and 3 (calcined at 873 K for 3 and 6 hours, respectively) is visibly narrowed as compared with the parent P-25 sample. It has previously been observed that Degussa P-25 consists of amorphous material, besides anatase and rutile [19]. It is unsurprising therefore, that an apparent transformation of the amorphous material to anatase, and thus an increase in crystallinity, were observed after calcination.

3.1.3. The variation of surface area and porosity with calcination

BET results for the surface area, pore size and pore volume are shown in Table II. The surface area of the parent P-25 powder is 54 m^2/g, which is in good agreement with a value of 55 m^2/g reported by Minero *et al*. [20], but larger than that reported by Sclafani *et al*. (44 m^2/g) [5]. Its pore volume is only 0.0246 m^3/g. Since uncalcined Degussa P-25 consists of agglomerates of crystallites [5], such a low porosity means that the surface area is largely external to the agglomerates and the pore volume measured is mainly located between the agglomerates (interagglomerate pores). At a temperature of 873 K, the surface area, pore size and pore volume only changed slightly for calcination between 3 and 6 hours. However, when the calcination took place for 24 hours, the surface area decreased by 20% and the pore size increased slightly. This could be interpreted as resulting from the fast intra-agglomerate densification or intercrystallite sintering within the agglomerates, since the XRD results showed that the mean crystallite size increased. Such sintering invariably leads to shrinking of the agglomerates and elimination of the small intercrystallite pores in the agglomerates and thus slightly increased the mean pore diameter. Wagner *et al*. also considered that the small pores inside the agglomerates have higher sintering rates [21].

TABLE II Nitrogen adsorption (BET) results for treated and untreated Degussa P-25

Calcination conditions		Surface area	Pore size	Pore volume
Temp. (°C)	Time (h)	(m^2/g)	(nm)	(m^3/g)
0	0	54.09 ± 0.39	1.829	24.7×10^{-3}
600	3	53.29 ± 0.53	1.828	24.4×10^{-3}
600	6	52.27 ± 0.68	1.836	24.0×10^{-3}
600	24	45.26 ± 0.39	1.902	21.5×10^{-3}
0	0	54.09 ± 0.39	1.829	24.7×10^{-3}
600	3	53.29 ± 0.53	1.828	24.4×10^{-3}
650	3	46.85 ± 0.55	1.833	21.5×10^{-3}
700	3	34.23 ± 0.42	1.829	15.7×10^{-3}
750	3	18.51 ± 0.23	1.825	8.4×10^{-3}
800	3	13.92 ± 0.28	1.796	6.3×10^{-3}
900	3	7.088 ± 0.16	1.761	3.1×10^{-3}
1000	3	3.978 ± 0.14	1.693	1.7×10^{-3}

When the calcination temperature exceeded 973 K, the surface area, pore size and pore volume began to decrease significantly. Specifically, the total porosity began to decrease rapidly above 1073 K. It is interesting to note that the changes observed in pore diameters for samples calcined above 973 K are comparatively small, whereas the pore volume and surface area differ by an order of magnitude. The pore volume and surface area of P-25 calcined at 1273 K (sample 10) were less than one tenth of the original values of the uncalcined powder. Such a decrease implied that further microstructural changes took place. TEM and XRD observations have shown that during calcination at higher temperatures, crystal growth and

(a)

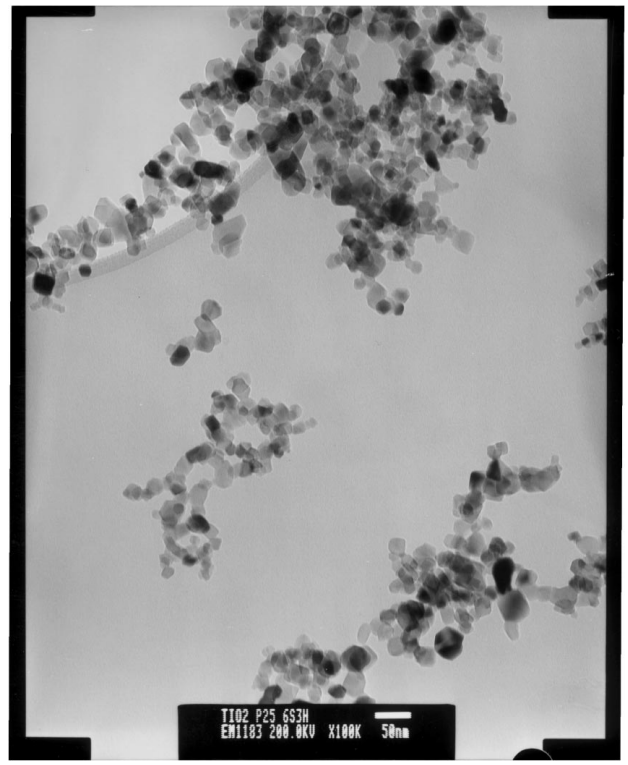

(b)

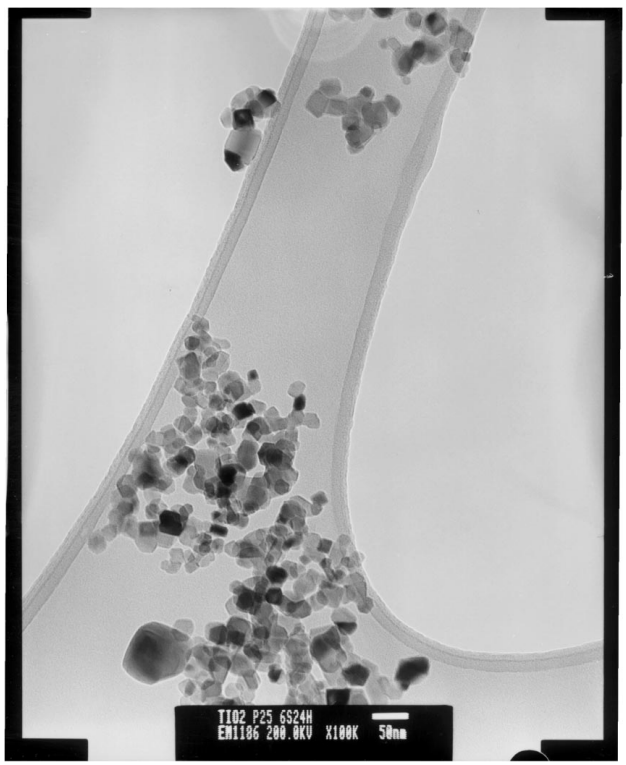

(c)

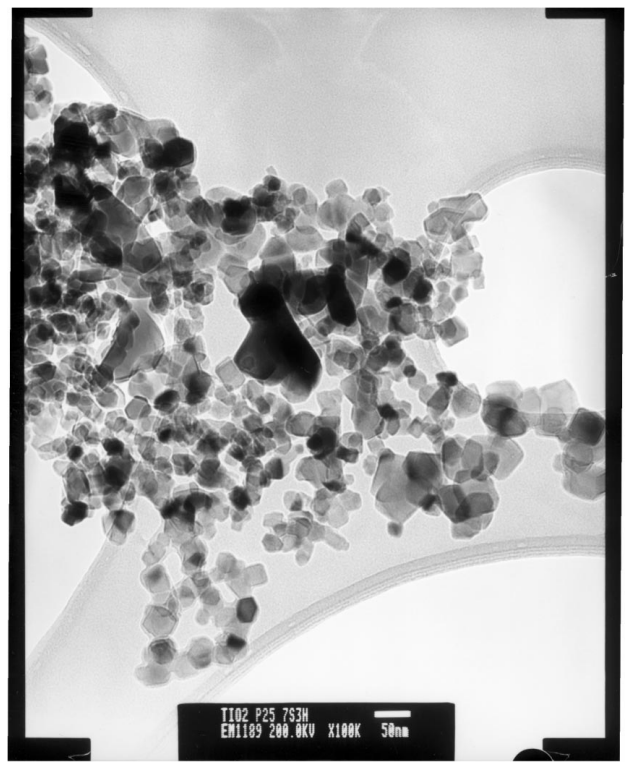

(d)

Figure 3 TEM Micrographs representative of the following samples: (a) Uncalcined P-25; (b) Calcined at 873 K for 3 hours; (c) Calcined at 873 K for 24 hours; (d) Calcined at 973 K for 3 hours; (e) Calcined at 1273 K for 3 hours. *(Continued)*

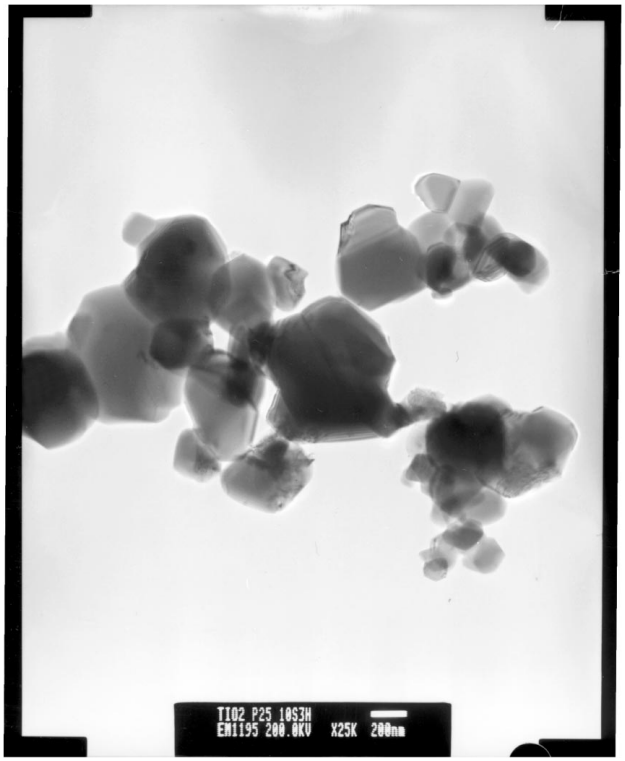

(e)

Figure 3 (Continued)

interagglomeration accompanied the phase transition. The development of the pore structure is determined largely by the degree of the agglomeration of the powders. With the crystal growth and the interagglomeration, the interagglomerate distance decreases and consequently the pore size distribution shifts to smaller pores. This means that the pore narrowing is a natural consequence of the marked increase observed in the grain size. In addition, the appreciable drop in pore volume is most likely attributable to destruction of the interagglomerate pores. This destruction could occur by physical collapse or flattening of the remaining pores as the interagglomeration proceeds, thus enclosing a significant portion of the pore making it inaccessible to nitrogen adsorption or condensation—resulting in a marked decrease in both the surface area and the pore volume. Hence the nitrogen adsorption results produced further support for the model proposed for phase transformation and grain growth of nanocrystalline titania [17].

3.2. The photocatalytic properties of Degussa P-25 TiO_2 samples

3.2.1. The effect of catalyst concentration on catalytic efficiency

An initial series of experiments were carried out using different amounts of P-25 TiO_2 as received, without calcination. The results are presented in Table III. Here, conversion is defined as the percentage of the original TOC that has disappeared after 2.5 hours reaction time in the reaction system employed here. The photocatalytic efficiency is defined as the conversion of TOC per hour and per gram of the catalyst per litre of suspension. The first experiment in Table III was performed without TiO_2 and a 14% reduction in TOC was achieved under these experimental conditions. This result indicates that some photolytic degradation occurred and thus any degradation observed for photocatalytic experiments may be as a result of both photolysis and photocatalysis. Other experiments were carried out using different catalyst concentrations and the results demonstrate that the nanocrystalline TiO_2 powders have high photocatalytic reactivity, as measured by phenol degradation. When the catalyst loading was only 0.15 g in 1.5 l of suspension, the TOC disappearance reached 64.4% in a reaction time of 2.5 hours. The TOC conversion was observed to increase with increasing TiO_2 loading until a plateau is reached at a concentration of over 0.5 g in 1.5 l of reaction solution, when light absorption by the suspension reached almost 100%. Unsurprisingly, these results indicate that when operating in a regime of high photon absorption, further increase in catalyst concentration results in little enhancement of the degradation efficiency since the light distribution within reactor becomes less homogeneous. This effectively restricts the photons to a very small region near the UV-lamp and under such conditions the small ratio of irradiated volume to total reactor volume is unfavourable for an efficient photochemical process [22].

TABLE III Effect of concentration of untreated Degussa P-25 on TOC removal

Mass of P-25 in 1.5 dm^3 of solution	Light intensity (mW/cm^2)	Percent TOC conversion	Efficiency (%TOC/dm^3 h g)
0.00	27.00	14.7 ± 3.8	—
0.15	3.40	64.4 ± 0.6	114.5
0.25	1.06	66.4 ± 1.2	70.8
0.50	0.12	74.6 ± 1.1	39.8
1.00	0.03	76.1 ± 0.5	20.3

3.2.2. The effect of catalyst composition and crystallinity on photoactivity

Photocatalytic degradation experiments were carried out using the samples calcined under different conditions and the results are listed in Tables III and IV.

TABLE IV Photocatalytic activity comparison of treated and untreated Degussa P-25

Calcination conditions		Light intensity	Percent TOC	Efficiency
Temp. (°C)	Time (h)	(mW/cm^2)	conversion	(%TOC/dm^3 h g)
0	0	1.06	66.4 ± 1.2	70.8
600	3	2.00	68.7 ± 1.1	73.3
600	6	1.40	64.9 ± 0.6	69.2
600	24	1.90	59.3 ± 1.4	63.3
0	0	1.06	66.4 ± 1.2	70.8
600	3	2.00	68.7 ± 1.1	73.3
650	3	2.50	74.5 ± 0.4	79.5
700	3	6.50	58.0 ± 1.6	61.9
750	3	7.50	26.5 ± 1.1	28.3
800	3	13.5	21.0 ± 2.0	22.4
900	3	15.5	16.5 ± 2.5	17.6
1000	3	16.0	11.8 ± 2.5	12.6

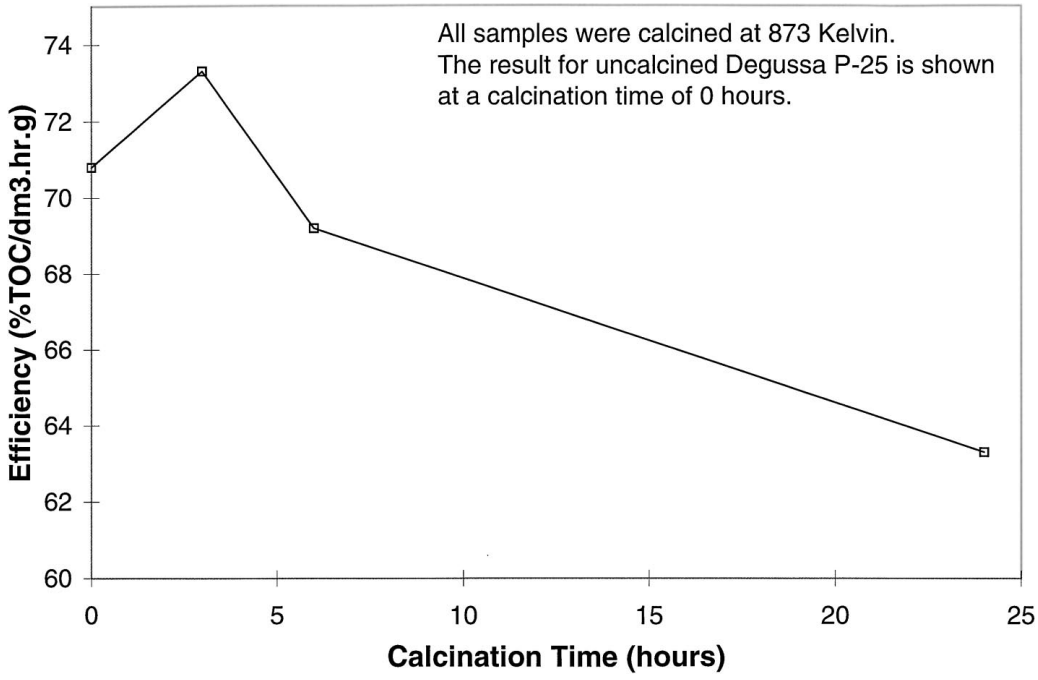

Figure 4 Effect of calcination time on phenol (TOC) degradation.

Fig. 4 shows the effect of calcination time on TOC conversion using the TiO_2 samples heat treated at 873 K. Only a slight change in photoactivity was observed for samples calcined for 3 and 6 hours (samples 2 and 3, respectively) although TOC conversion was significantly reduced for the sample calcined for 24 hours (sample 4). This is in agreement with the XRD and BET results mentioned previously in that there was only significant increase in the rutile content and decrease in the surface area observed for the sample calcined for a long time (see Table I). It appears that the distinction between both crystal structure and surface are effects on TOC conversion is difficult, however, comparing the sample 4 with sample 5 (calcined at 923 K), both have a similar value of surface area (45.26 m^2/g and 46.85 m^2/g), but the latter has a lower rutile content (28.7% versus 38.1%) and reveals higher conversion (74.5% versus 59.3%). Several previous reports have mentioned that the anatase form of TiO_2 has somewhat larger band-gap energy than rutile ($E_g = 3.23$ versus 3.02 eV, respectively) and shows a higher reactivity. Rutile is also believed to be a relatively poor photocatalyst due to its higher electron-hole recombination rate [23–25]. Thus we can tentatively conclude that the lower activity of the sample 4 is more likely attributable to an increase in rutile content in the sample rather than the reduction in surface area.

Fig. 5 shows the photoreactivity of P-25 TiO_2 calcined for 3 hours at different temperatures. From 873 to 923 K, calcination resulted in an increase in activity and P-25 calcined at 923 K revealed the highest activity of the conditions examined. BET and XRD results indicate that the surface area decreases, the rutile content increases and the anatase crystallite size and crystallinity increase as the calcination temperature increases from 873 to 923 K. The observed rate enhancement cannot be explained by the change in surface area and rutile content and we believe it is primarily due to an improvement in crystallinity, shown by XRD. Similar improvements in photoactivity have been obtained for other titania powders fired at a temperatures lower than 923 K [5].

3.2.3. The effect of crystallite size on photoactivity

Fig. 5 also shows that, for those samples calcined at temperatures greater than 923 K, photoactivity decreases with increasing calcination temperature. XRD and TEM measurements have indicated that at temperatures exceeding 973 K, phase transformation and sintering proceeded rapidly. The former process increased the proportion of the inactive rutile phase and the latter increased the grain size. Larger grain sizes resulted in increased light transmission since densification of the agglomerates made the powder more difficult to disperse and the data shown in Fig. 6 support this. Thus increasing calcination temperature resulted in reduced utility of UV light and lowered photocatalytic efficiency. For P-25 calcined at 1273 K (sample 10), the TOC conversion observed was only 11.8%—indicating that its absorption of the shorter wavelength UV radiation (responsible for the photolytic reaction) was not compensated for by the material's low photocatalytic activity. Thus the TOC conversion observed was lower than that due to photolysis alone.

4. Summary

The microstructure characteristics of Degussa P-25 TiO_2 calcined under different conditions have been studied using XRD, BET, and TEM. Their photoreactivities were also evaluated using phenol mineralisation as a test reaction. The results indicated that after calcination at 873 K for 3 hours and 6 hours the

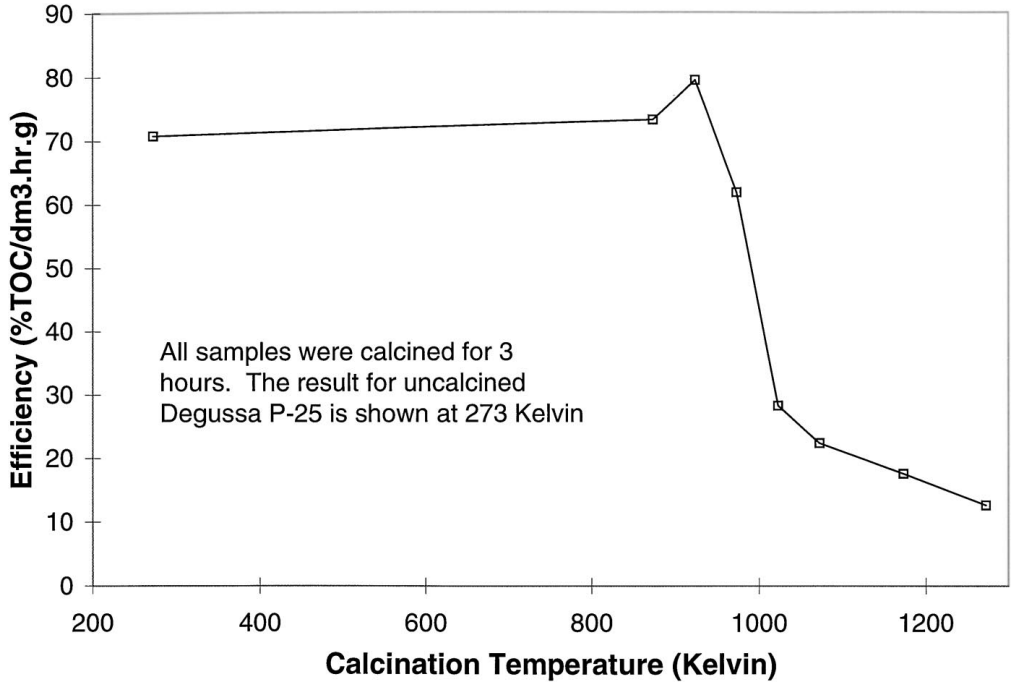

Figure 5 Effect of calcination temperature on phenol (TOC) degradation.

structure parameters did not change significantly, but after 24 hours at the same temperature, the rutile content obviously increased. As the calcination temperature increased beyond 973 K the crystal size, rapid increase in the rutile content and reduction in the surface area were observed. The photocatalytic activity of the samples showed that for the sample treated at 873 K for 3 and 6 hours, the photoreactivities do not show much difference against the activity of the uncalcined TiO_2 powder, but decreased for the sample calcined for 24 hours. At temperatures greater than 973 K, the photocatalytic activity decreased significantly with calcination temperature. The sample calcined at 923 K for 3 hours showed the highest degradation efficiency under the conditions employed in this study.

This study has provided some additional insight into the reasons for photocatalytic activity or inactivity of heat treated Degussa P-25 titania. Of the many microstructure characteristics that may affect photoactivity—such as the surface crystallinity, crystal size, rutile content—most were subject to reasonably large variations over the range of treatment conditions employed. Although it was not possible to completely decouple the effects of each of the different parameters, the results presented here appear to indicate dependence of photocatalytic reactivities on certain microstructure characteristics. Among those factors examined, anatase crystallinity and grain size have been observed to be important. Conversely the effects of prolonged calcination and calcination at high temperatures are detrimental to the photocatalytic activity of Degussa P-25.

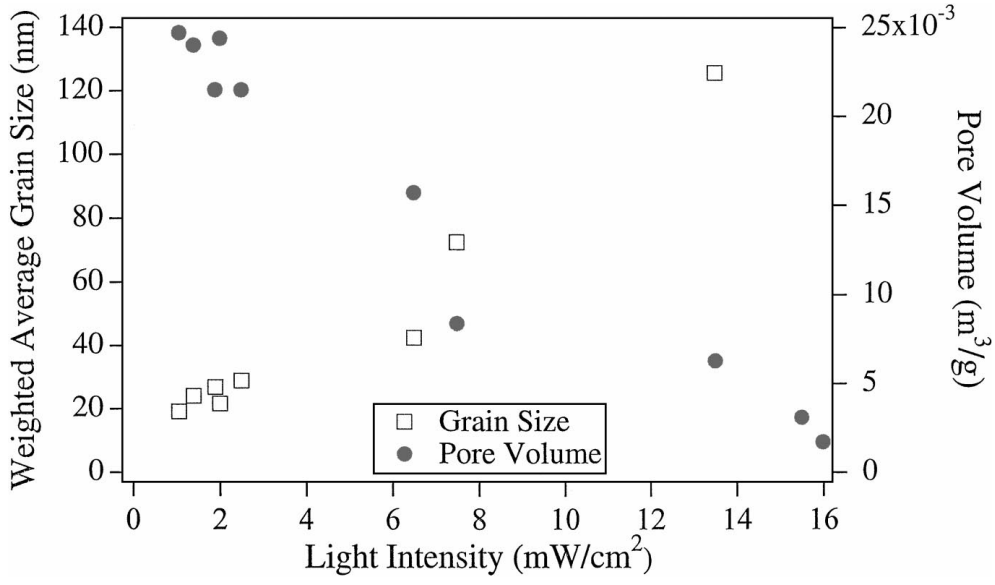

Figure 6 Variation of pore volume and average grain size with transmitted light intensity.

Acknowledgements

The financial support of the Hong Kong Research Grants Council, through grant HKUST 582/94E, is gratefully acknowledged.

References

1. M. A. FOX and M. T. DULAY, *Chem. Rev*. **93** (1993) 341.
2. A. L. LINSEBIGLER, G. Q. LU and J. T. YATES, JR., *ibid*. **95** (1995) 735–758.
3. A. P. RIVERA, K. TANAKA and T. HISANAGA, *Appl. Catal. B: Environmental* **3** (1993) 37.
4. H. M. DIX, "Environmental Pollution" (Wiley, New York, 1981) p. 110.
5. A. SCLAFANI, L. PALMISANO and M. SCHIAVELLO, *J. Phys. Chem*. **94** (1990) 829.
6. D. F. OLLIS, *Environ. Sci. Technol*. **19** (1985) 480.
7. R. W. MATTHEWS, *Water Res*. **24** (1990) 653.
8. H. AL-EKABI, N. SERPONE, E. PELIZZETTI, C. MINERO, M. A. FOX and R. B. DRAPER, *Langmuir* **5** (1989) 250.
9. C. TURCHI and D. F. OLLIS, *J. Catal*. **122** (1990) 178.
10. M. ANPO, T. SHIMA, S. KODAMA and Y. KUBOKAWA, *J. Phys. Chem*. **91** (1987) 4305.
11. R. W. MATTHEWS, *Pure Appl. Chem*. **64** (1992) 1285.
12. X.-Z. DING, X.-H, LIU and Y.-Z. HE, *J. Mater. Sci. Lett*. **15** (1996) 1789.
13. D. D. BECK and R. W. SIEGEL, *J. Mater. Res*. **7**(10) (1992) 2840.
14. R. I. BICKLEY, J. S. LEES, R. J. D. TILLEY, L. PALMISANO and M. SCHIAVELLO, *J. Chem. Soc. Faraday Trans*. **88**(3) (1992) 377.
15. R. D. SHANNON and J. A. PASK, *J. Amer. Ceram. Soc*. **48**(8) (1965) 391.
16. B. D. CULLITY, "Elements of X-Ray Diffraction," 2nd ed. (Addison-Wesley, Reading, WA, 1978) p. 94.
17. D. C. HAGUE and M. J. MAYO, *Nanostructured Materials* **3** (1993) 61.
18. L. H. EDELSON and A. M. GLAESER, *J. Amer. Ceram. Soc*. **71** (1988) 225.
19. R. I. BICKLEY, T. GONZALEZ-CARRENO, J. S. LEES, L. PALMISANO and R. J. D. TILLEY, *J. Solid State Chem*. **92** (1991) 178.
20. C. MINERO, F. CATOZZO and E. PELIZZETTI, *Langmuir* **8** (1992) 481.
21. W. WAGNER, R. S. AVERBACK, H. HAHN, W. PETRY and A. WIEDENMANN, *J. Mater. Res*. **6**(10) (1991) 2193.
22. M. PASQUALI, F. SANTARELLI, J. F. PORTER and P.-L. YUE, *AIChE J*. **42**(2) (1996) 532.
23. B. KRAEUTLER and A. J. BARD, *J. Amer. Chem. Soc*. **100** (1978) 5985.
24. K. OKAMOTO, Y. YAMAMOTO, H. TANAKA, M. TANAKA and A. ITAYA, *Bull. Chem. Soc. Jpn*. **58** (1985) 2015.
25. S. NISHIMOTO, B. OHTANI, H. KAJIWARA and T. KAGIYA, *J. Chem. Soc., Faraday Trans. 1* **81** (1985) 61.

Received 3 November 1997
and accepted 11 November 1998